

Two-way FSI modelling of blood flow through CCA accounting on-line medical diagnostics in hypertension

K Czechowicz^{1,2}, J Badur¹, K Narkiewicz²

¹ Energy Conversion Department, Institute of Fluid-Flow Machinery PAS-ci, Gdańsk, Poland

² Medical University of Gdańsk, Gdańsk, Poland

E-mail: krzysztof-czechowicz@gumed.edu.pl

Abstract. Flow parameters can induce pathological changes in the arteries. We propose a method to assess those parameters using a 3D computer model of the flow in the Common Carotid Artery. Input data was acquired using an automatic 2D ultrasound wall tracking system. This data has been used to generate a 3D geometry of the artery. The diameter and wall thickness have been assessed individually for every patient, but the artery has been taken as a 75mm straight tube. The Young's modulus for the arterial walls was calculated using the pulse pressure, diastolic (minimal) diameter and wall thickness (IMT). Blood flow was derived from the pressure waveform using a 2-parameter Windkessel model. The blood is assumed to be non-Newtonian. The computational models were generated and calculated using commercial code. The coupling method required the use of Arbitrary Lagrangian-Euler formulation to solve Navier-Stokes and Navier-Lamè equations in a moving domain. The calculations showed that the distention of the walls in the model is not significantly different from the measurements. Results from the model have been used to locate additional risk factors, such as wall shear stress or circumferential stress, that may predict adverse hypertension complications.

1. Introduction

Cardiovascular diseases are becoming the main cause of death and disabilities in the modern world [1]. Treatment for some of the diseases like hypertension is expensive and mostly concentrates on managing the disease [2]. Identifying the early onsets and biological mechanisms leading to the end result is becoming an urging challenge and more detailed research is needed. The focus of this paper is on providing a tool to extract mechanical details of the cardiovascular system, that have not been available up to date. Scientists tried to extract mechanical parameters from the human body since the beginning of modern mechanics. Earliest work regarding the effects of the interaction between blood and the walls of the arteries can be dated to work by Thomas Young from 1808 [3]. Since then many analytical and numerical solutions have been proposed but the computational power of modern computers allows acquiring very detailed information about flow in the arteries.

It is known that the blood vessels react to the flow in many ways. The reactions can be short-term, such as aligning of the cells on the inner most layer of the wall [4], or releasing ATP (Adenosine triphosphate) [5] and long-term such as permanent increase in diameter or vessel wall thickness [6]. The main mediator of these changes is thought to be the Wall Shear Stress (WSS) generated by the pulsate flow of blood, and blood pressure. In a pulsate flow, calculation of the WSS is very problematic and it cannot be measured due to lack of precision of modern medical devices.



Furthermore blood flow is pulsate and as such the profile is not always parabolic, but acts according to the Womersley solution of pulsate flows [7]. Therefore use of computer modelling is the best alternative. The way blood pressure changes within one heart cycle varies between patients, therefore to analyze the problem in detail, a series of patient specific models have to be created.

Most work done in this field focuses on using Magnetic Resonance Imaging or Computed Tomography [8][9]. Those imaging methods are expensive, time consuming and may be harmful to the patient, which excludes the use of this method on a significant number of patients. In this paper we present a method of generating patient specific computational models of the human Common Carotid Artery (CCA) based on data acquired during an ultrasound examination of the arteries.

2. Anatomy

Humans have four arteries that supply blood to the head. Two Common Carotid Arteries go through the front of the neck on either side. These are the main suppliers of blood to the brain and other intracranial organs. In the upper neck arteries bifurcate to form internal and external carotid arteries.

The walls of the arteries are build of 3 layers. The inner most is called Intima and it consists of a single layer of endothelial cells. The middle layer is Media and it consists of smooth muscle cells and connective elastic tissue. It is responsible for most of the artery's thickness and mechanical properties. The outer most layer, Adventitia, is mostly built of connective tissue and its main function is supporting the artery. The complex of Intima and Media is the main pressure load bearing part of the artery. Furthermore the interfaces between the artery's lumen and intima, as well as the interface between Media and Adventitia are visible on ultrasound images. Their thickness is often used as a measure of artery thickness and is referred to as Intima Media Thickness (IMT)

3. Methods

We studied a group of 18 people with high normal blood pressure and early detected hypertension. Mean age of our patients was 36 (± 10) years. The patients had never been treated for hypertension and had not been diagnosed with any other chronic diseases. All of our measurements were non-invasive and were carried out in supine position in a quiet room after a 15 minute rest. The measurements have been conducted on the right CCA. The exact spot was found by locating the CCA bifurcation and placing the start of it at the distal edge of the ultrasound image.

3.1. Data acquisition

The ultrasound machine used in this study was an Esaote Picus Pro device equipped with a prototype wall tracking system ART.LAB (Esaote, Maastricht, Netherlands). The system provides very high resolution images, with a pixel size of $23\mu\text{m} \times 23\mu\text{m}$, and a very high frame rate of 600Hz. The wall tracking system provides continuous recordings of the distention of the artery, its diameter and IMT. Data is recorded in 14 lines perpendicular to the probe. Simultaneously other biological signals were recorded. Continuous blood pressure waveform was obtained from the finger using the Finometer device (Finapres Medical Systems, Amsterdam, The Netherlands) linked to a PowerLab (ADInstruments, Dunedin, New Zealand) data acquisition system which also recorded electrocardiograms (ECG). The ECG and blood pressure signals were synchronised automatically with each other. The ECG signal was duplicated and sent to the ART.LAB device and recorded along with the ultrasound data. This was used to synchronise the signals in pre processing.

3.2. Data Preprocessing

Due to the high resolution of the data the length of the ultrasound recordings is limited to 4.7 seconds thus a series of 5-10 measurements were carried out. In order to achieve maximum accuracy ultrasound recordings had to be synchronised with the BP recording. The ECG signal recorded along with the ultrasound dataset was fitted to a window of 10 seconds around the start of the ultrasound measurement.

For each patient recording of one heart beat was selected. The criteria for this selection was the minimum difference between the distention waveforms taken from different ultrasound lines, as well as no interruptions, such as calibration, on the blood pressure recording.

3.2.1. Pressure waveform

Knowing the blood pressure measured in the finger and the distention of the carotid artery it is possible to estimate local pressure in the artery. Arterial pressure is characterized by two main values: Systolic Blood Pressure (SBP) – the maximum pressure in a heartbeat and Diastolic Blood Pressure (DBP) – the minimum blood pressure. Experimentally it is well established [10] that the value of DBP is constant throughout the arterial tree in each heartbeat. The same is true for a value called Mean Arterial Pressure (MAP) calculated as (1)

$$\text{MAP} = \frac{1}{3}\text{SBP} + \frac{2}{3}\text{DBP} \quad (1)$$

The local pressure waveform is estimated by scaling the distention waveform according to (2) where the scaling factor is given by (3) assuming that the wall of the artery to have linear elastic properties.

$$p(t) = \delta \cdot D(t) + \text{DBP} \quad (2)$$

$$\delta = \frac{\text{MAP} - \text{DBP}}{\bar{D}} \quad (3)$$

where \bar{D} is the average distention calculated over the whole heartbeat.

3.2.2. Young's modulus

The arterial wall is considered to be linear elastic and incompressible therefore it has a constant Young's modulus for each patient and Poissons number of $\nu = 0.5$. For numerical purposes a value of $\nu = 0.495$ was taken. As for the Young's modulus a value for each patient was calculated as

$$E = \frac{(1 - \nu^2)D}{\text{IMT} \cdot \text{DC}} \quad (4)$$

Where DC is the distensibility coefficient given by

$$\text{DC} = \frac{2D \cdot \Delta D + \Delta D^2}{D^2 \cdot \Delta p} \quad (5)$$

Young's modulus defined in such a way takes into account material properties of the entire vessel wall. It is worth mentioning that the value is not representative for the elasticity of both the Media and Intima layers of the artery separately, but it is a surrogate value for the entire vessel including the adventitia layer. Furthermore it is a linear approximation of the real elasticity of the vessel.

3.2.3. Pulse wave velocity

Blood travels through the arterial tree in a pulsate manner. Each pulse travels at a velocity given by the Moens Korteweg [11] equation in a form modified by Bramwell [12]

$$\text{PWV} = \sqrt{\frac{dp \cdot V}{d \cdot \rho}} \quad (6)$$

After introducing the distensibility coefficient (5)

$$\text{PWV} = \frac{1}{\sqrt{\rho \cdot \text{DC}}} \quad (7)$$

The local PWV in the CCA can reach values between 4m/s and 10m/s, which means the pulse needs between 0.0075s and 0.01875s.

3.2.4. Mass Flow

Mass flow of blood was obtained by using a zero dimensional two parameter Windkessel model proposed by Frank in 1899 [13].

$$\dot{m} = \frac{p(t)}{R} + C \frac{dp}{dt} \quad (8)$$

Parameter R represents the mean resistance of the arteries and can be easily calculated when the amount of blood flowing through the artery in every heartbeat is known. Parameter C for this model is obtained by solving equation (8) in a period after the heart has finished contracting when the flow in the artery is expected to be stable.

4. Computer model

Data prepared as described above has been used to create transient computational models of momentum exchange between the fluid (blood) and the solid (arterial walls). The model has been prepared in the ANSYS Workbench environment. The fluid domain was solved using the CFX solver and the solid domain was solved using the ANSYS Mechanical solver. Each of these solvers is based on a different discretisation method. CFX uses the finite volume method and ANSYS Mechanical is using the finite element method. Communication between the solvers was provided by ANSYS Workbench.

4.1. Fluid domain

The fluid part of the model was computed by the CFX finite volume solver. The governing equations for this software are the Navier-Stokes equations. These in general consist of three laws of conservation: conservation of mass, momentum and energy (11) [14]. The conservation equations used in the Arbitrary-Lagrangian Eulerian formulation to accommodate for the moving mesh. The formulation is obtained by subtracting the velocity of the mesh from fluid velocity in the convective flux of the standard formulation.

$$\partial_t \begin{Bmatrix} \rho \\ \rho \vec{v} \\ \rho e \end{Bmatrix} + \text{div} \begin{Bmatrix} \rho(\vec{v} - \vec{w}) \\ \rho \vec{v} \otimes (\vec{v} - \vec{w}) \\ \rho e(\vec{v} - \vec{w}) \end{Bmatrix} + \begin{Bmatrix} 0 \\ p \vec{I} \\ p \vec{v} \end{Bmatrix} = \text{div} \begin{Bmatrix} 0 \\ \vec{\tau}^c \\ \vec{\tau}^c \vec{v} + \vec{q}^c \end{Bmatrix} + S \quad (9)$$

This can be written in a different form, reviling the fluxes

$$\partial_t \{ \mathbf{u} \} + \text{div} \{ \mathcal{F}^c \} + \{ \mathcal{F}^e \} = \text{div} \{ \mathcal{F}^v \} + S \quad (10)$$

In this case there is no transfer of energy within the domain, as the temperature is assumed to be constant; therefore the latter equation is always fulfilled. Blood is considered to be incompressible therefore its density is constant. Implementing those changes simplifies the conservation equations (9) to the form of Navier-Stokes equations.

$$\begin{aligned} \nabla \cdot \vec{v} &= 0 \\ \rho \left(\frac{\partial \vec{v}}{\partial t} + \vec{v} \cdot \nabla \vec{v} \right) + \nabla p &= \mu \nabla^2 \vec{v} \end{aligned} \quad (11)$$

where \vec{v} is blood velocity, ρ is density, μ is blood viscosity.

The domain has been divided into a structural mesh swept along the length of the vessel with 6 layers of inflating near the arterial wall. The same settings have been used for each patient to increase automatization of the calculation process.

4.2. Solid domain

The solid part of the model has been solved by the ANSYS Mechanical solver. The walls have been modelled by one layer of 3 dimensional elements. The size of the elements has been chosen to be as close to proportions of 1:1:2 as possible, with the elongation in the axial direction. The total number of elements was around 800. This value was proven to be sufficient in several numerical experiments carried out by our team. The governing equations for this solver are the Navier-Lame equation

$$\sigma = 2\mu \epsilon + \lambda \text{tr} \epsilon \mathbf{I} \quad (12)$$

The distention of the artery is expected to be around 8% of the diameter, reaching up to 14%. The scale of deformations of the walls of the artery required using the finite deformation approach. This means that the elements of the Green's Tensor (13) had to be taken in full form, as its final term is expected to have non negligible values

$$\epsilon_{ij}^G = \frac{1}{2} \left(\frac{\partial u_i}{\partial x_j} + \frac{\partial u_j}{\partial x_i} + \frac{\partial u_k}{\partial x_i} \frac{\partial u_k}{\partial x_j} \right) \quad (13)$$

4.3. Fluid Solid Interaction

As mentioned before the solid and fluid domains are solved in separate programs using different methods. Coupling between them has to insure that the forces acting between the domains (14), and the deformation of the domains (15) are equal. We achieved this using the conservation of momentum method.

$$\left(\mathcal{F}^c - \mathcal{F}^e \right) \cdot \mathbf{n}|_{\text{solid}} = \left(\mathcal{F}^c - \mathcal{F}^e \right) \cdot \mathbf{n}|_{\text{fluid}} \quad (14)$$

$$\vec{v}|_{\text{solid}} = \vec{v}|_{\text{fluid}} \quad (15)$$

where \mathbf{n} are versors normal to the boundary in solid and fluid.

Movement of the mesh has been described by the use of the Laplace equation (16). It is also necessary that the velocity of the mesh near the wall is equal to the velocity of the wall, to avoid creating a gap (17).

$$\text{div}[(1 - \alpha)\text{grad } \vec{w}] = 0 \quad (16)$$

$$\vec{w}|_{\text{CS}} = \vec{v}|_{\text{fluid}} \quad (17)$$

The stiffness coefficient α in equation (16) has been set to increase near the boundaries where thinner elements are located.

4.4. The model

The arteries have been modelled as straight tubes with the diameter and wall thickness measured by the ART.LAB system. The walls at inlet and outlet have been fixed, to prevent the movement of the artery and allow implementation of the boundary conditions to the fluid domain. This means that when the artery is distended nozzles appear at both ends. We found empirically, by testing different lengths of the model, that the influence of the inlet nozzle is observable only within the first 40mm. The outlet nozzle has only local effects in the flow. Therefore the most optimal length of the model is 75mm with only the part between the 40th and 65thmm taken into further analysis.

For the fluid domain we applied an opening type boundary on the inlet side, to allow the fluid to flow both in and out of the domain. The boundary is governed by flow in the axial direction. The outlet boundary has been set as a pressure boundary condition. As mentioned earlier the pulse travels through the arteries with a finite velocity. The model has a time step of 0.005s and, as mentioned in paragraph 3.2.3, the time necessary for the pulse to travel through the artery can be up to 0.019s. To compensate for the delay conditions an offset at the inlet boundary condition given by the time calculated from equation (7) has been implemented.

Blood has been modelled as an incompressible non Newtonian fluid. The viscosity of the blood has been modelled using the power law expression (18). The properties for this model have been taken from literature [15]. According to Neofytou this model takes into account both viscous and two-phase properties of blood.

$$\mu = K \cdot (\dot{\gamma})^n \quad (18)$$

where $K = 146.7 \text{ mPas}^n$ and $n = 0.7755$. Elastic material properties for the vessel wall have been calculated individually for each patient.

5. Results

After each calculation, the results have been inspected manually to verify that the calculated distention waveform is the same as the measured distention waveform used as input. A sample comparison is depicted on Figure 1. The distention is caused by total pressure, a sum of static pressure and dynamic pressure. the latter is a result of the blood velocity. Similarity of the input and output data, shows that the total pressure of blood in the model is the same as that in the artery. Thus the velocity is the same as well.

In all cases an additional high frequency component is visible on the calculated results. This component is a consequence of limitations of the 2-element Windkessel method used to obtain the input velocities. Using a higher order of the Windkessel model would help solve it, however it is impossible to obtain additional parameters needed for them. Nevertheless the scale of this disturbance is much smaller than the scale of the distention.

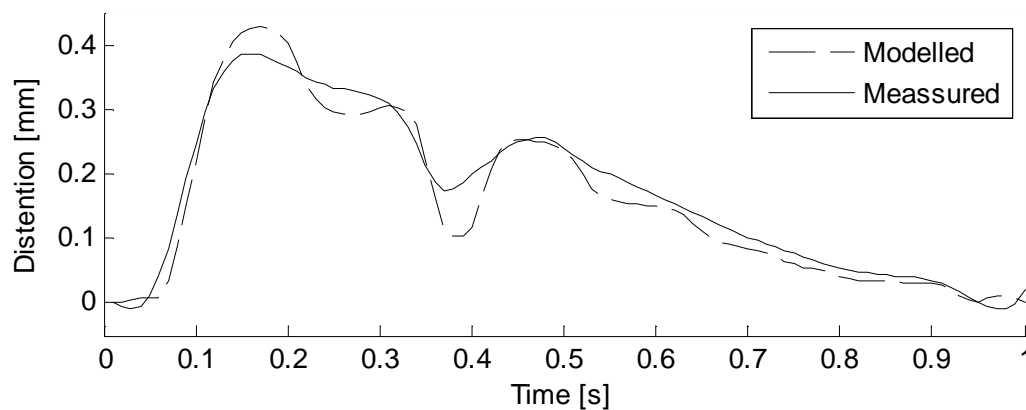


Figure 1. Comparison between the distention of the model versus measurements.

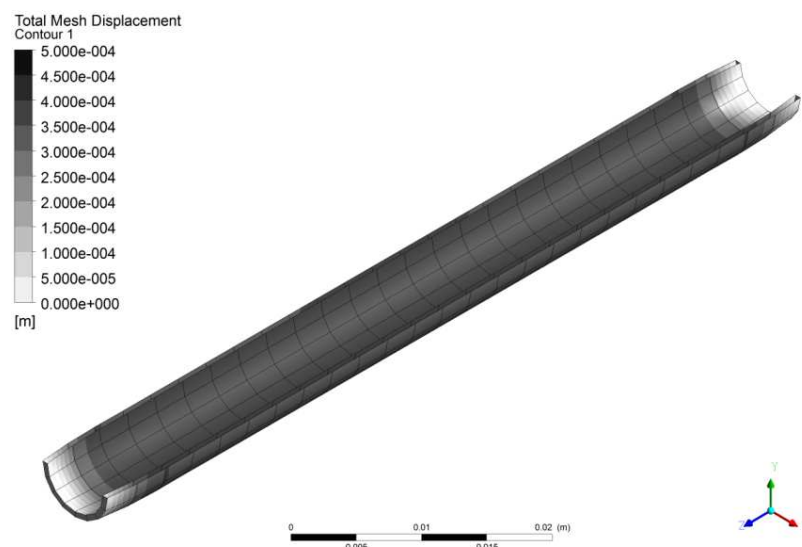


Figure 2. Half of the fully deformed model, presenting total mesh displacement

The deformation of the model can be seen on the images of the full model. Figure 2 shows the full model length with mesh on the surface. The maximal deformation of this model is 0.4 mm. This means that the deformation is over 10%. (the radius of the artery is 3mm).

One of the main results is obtaining transient maps of wall shear stress (Figure 3). High values of the WSS are considered a risk factor in many cardiovascular diseases. Identifying those patients will help with administering preventive treatment, to stop development of cardiovascular problems.

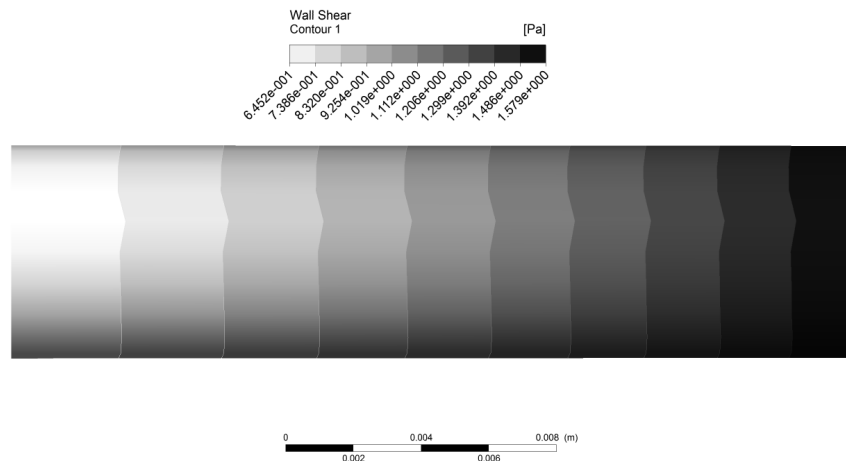


Figure 3. Example Wall Shear Stress map of the model

6. Conclusion

The results of this work show that the approach proposed in this paper is validated and can be used in further medical research on larger groups of patients. High automatization of model preparation reduces labour input needed from the researcher for each patient, making it a viable method for large cohort research.

The method has been developed to work with fully 3 dimensional geometries, therefore it is possible to apply this approach to more complex geometries.

7. Reference

- [1] Nichols M, Townsend N, Luengo-Fernandez R, Leal J, Gray A, Scarborough P and Reyner M 2012 *European Cardiovascular Disease Statistics 2012*. European Society of Cardiology, Sophia Antipolis (European Heart Network, European Society of Cardiology, Sophia Antipolis)
- [2] Mancia G, et al 2013 2013 ESH/ESC Guidelines for the management of arterial hypertension: The Task Force for the management of arterial hypertension of the European Society of Hypertension (ESH) and of the European Society of Cardiology (ESC) *J. Hypertens.* **31** 1281–357
- [3] Young T 1808 Hydraulic Investigations, Subservient to an Intended Croonian Lecture on the Motion of the Blood *Philos. Trans. R. Soc. Lond.* **98** 164–86
- [4] Topper J N and Gimbrone Jr M A 1999 Blood flow and vascular gene expression: fluid shear stress as a modulator of endothelial phenotype *Mol. Med. Today* **5** 40–6
- [5] Bodin P and Burnstock G 2001 Evidence that release of adenosine triphosphate from endothelial cells during increased shear stress is vesicular *J. Cardiovasc. Pharmacol.* **38** 900–8

- [6] Boutouyrie P, Bussy C, Lacolley P, Girerd X, Laloux B and Laurent S 1999 Association Between Local Pulse Pressure, Mean Blood Pressure, and Large-Artery Remodeling *Circulation* **100** 1387–93
- [7] Womersley J R 1955 Method for the calculation of velocity, rate of flow and viscous drag in arteries when the pressure gradient is known *J. Physiol.* **127** 553–63
- [8] Reymond P, Crosetto P, Deparis S, Quarteroni A and Stergiopoulos N 2013 Physiological simulation of blood flow in the aorta: Comparison of hemodynamic indices as predicted by 3-D FSI, 3-D rigid wall and 1-D models *Med. Eng. Phys.* **35** 784–91
- [9] Moireau P, Xiao N, Astorino M, Figueroa C A, Chapelle D, Taylor C A and Gerbeau J-F 2012 External tissue support and fluid–structure simulation in blood flows *Biomech. Model. Mechanobiol.* **11** 1–18
- [10] Pauca A L, Wallenhaupt S L, Kon N D and Tucker W Y 1992 Does radial artery pressure accurately reflect aortic pressure? *CHEST J.* **102** 1193–8
- [11] Korteweg D J 1878 Ueber die Fortpflanzungsgeschwindigkeit des Schalles in elastischen Röhren *Ann. Phys. Chem.* **241** 525–42
- [12] Bramwell J C and Hill A V 1922 The Velocity of the Pulse Wave in Man *Proc. R. Soc. B Biol. Sci.* **93** 298–306
- [13] Sagawa K 1990 Translation of Otto frank’s paper “Die Grundform des arteriellen Pulses” zeitschrift für biologie 37: 483–526 (1899) *J. Mol. Cell. Cardiol.* **22** 253–4
- [14] Badur J 2005 *Pięć wykładów ze współczesnej termomechaniki płynów* (Gdańsk)
- [15] Neofytou P and Tsangaris S 2006 Flow effects of blood constitutive equations in 3D models of vascular anomalies *Int. J. Numer. Methods Fluids* **51** 489–510

Acknowledgments

This research was carried out as part of the TEAM project: „Integrated measurement of arterial function and sympathetic nervous system activity: development, validation and application of a new method” which was realized within the programme Innovative Economy of Foundation for Polish Science, co financed from European Union, Regional Development Fund